International Journal of Pharmaceutics 379 (2009) 167–173

Contents lists available at ScienceDirect

International Journal of Pharmaceutics

journal homepage: www.elsevier.com/locate/ijpharm

Pharmaceutical Nanotechnology

Development of a chemically stable 10-hydroxycamptothecin nanosuspensions

Xiaohui Pu[a], Jin Sun[a], Yan Wang[a], Yongjun Wang[a], Xiaohong Liu[a], Peng Zhang[a], Xing Tang[a], Weisan Pan[a], Jihong Han[b], Zhonggui He[a,*]

[a] Department of Biopharmaceutics, School of Pharmacy, Shenyang Pharmaceutical University, No. 103, Wenhua Road, Shenyang 110016, China
[b] Institute for Science and Technology in Medicine and School of Pharmacy, Keele University, Staffordshire, ST5 5BG, UK

ARTICLE INFO

Article history:
Received 21 March 2009
Received in revised form 24 May 2009
Accepted 28 May 2009
Available online 6 June 2009

Keywords:
Anticancer drugs
10-Hydroxycamptothecin
Nanosuspensions
Microprecipitation–high-pressure homogenization
Chemical stability improvement

ABSTRACT

The purpose of this study was to prepare and characterize nanosuspensions loading the active lactone form of 10-hydroxycamptothecin (10-HCPT). Nanosuspensions were prepared in terms of microprecipitation–high-pressure homogenization method. As for the preparation processes, three important parameters, i.e. the agitation rate of stabilizer solution, homogenization pressure and cycle numbers, were investigated and optimized, and the optimal values were 1000 rpm, 1000 bar and 20 times, respectively. The particle size and zeta potential of the 10-HCPT-nanosuspensions were 131 nm and −25.5 mV. The particle morphology was determined by transmission electron microscopy and the 10-HCPT nanoparticles were baculine or trabecular in shape. The solid state of 10-HCPT in nanoparticles was analyzed using X-ray powder diffraction (XRD) and differential scanning calorimetry (DSC). The XRD and the DSC results both indicated that 10-HCPT was present as an amorphous state in the lyophilized powders for nanosuspension. The chemical stability tests demonstrated that near 90% lactone form of 10-HCPT was present in the nanosuspensions but it was easily transferred to the carboxylate form in the solution at pH 7.0–8.0. In vitro dissolution tests showed the dissolution rate of nanosuspensions, compared with the coarse suspensions, had been significantly increased.

1. Introduction

Camptothecin (CPT) is a natural indole alkaloid extracted from a Chinese tree, Camptotheca Acuminata Decne in the 1960s (Wall et al., 1966). Due to the promising and potent anti-tumor activity, CPT and its derivatives including 7-ethyl-10-hydroxycamptothecin (SN-38), 10-hydroxycamptothecin (10-HCPT), 9-nitro-camptothecin, topotecan and irinotecan, have received more and more attention recently. The anti-tumor mechanism of these compounds is based on the inhibition of DNA replication and RNA transcription by stabilizing the cleavable complexes formed between topoisomerase I and DNA (Hsiang et al., 1985). All the CPT analogues can exist in two conformations: the carboxylate and lactone forms. The lactone form is the more effective inhibitor of topoisomerase I compared with the carboxylate form (Slichemeyer et al., 1993).

10-HCPT has shown the most strong anti-tumor effects among its analogues (Wall et al., 1966), and less toxic in experimental animals and in human trials compared to CPT (Han, 1994). It has been widely used in the treatment of gastric carcinoma, hepatoma, leukemia, and tumor of head and neck in clinical trials. Unfortunately, it has poor solubility in water and physiologically acceptable organic solvents, and its lactone ring readily opened and was completely converted into the carboxylate form under physiologic and alkaline condition (Fig. 1). Due to the poor solubility of the lactone form, 10-HCPT is usually used in the more soluble form of carboxylate salt which is more toxic and less active. In order to develop high performance delivery systems for the insoluble lactone form 10-HCPT, pharmaceutical scientists have made a lot of efforts to develop, such as microspheres (Shenderova et al., 1997, 1999; Lu and Zhang, 2006), nanoparticles (Sun et al., 2004; Zhang et al., 2006a, 2007a; Guo et al., 2007; Yang et al., 2007), niosomes (Shi et al., 2006; Hong et al., 2009), emulsions (Zhao et al., 2007), polymeric micelle systems (Zhang et al., 2007b) and prodrugs (He et al., 2004; Wang et al., 2005). However, these delivery systems also have some obvious limitations, such as low drug loading capacity, adverse effects induced by excipients or solvents, variability of effect and unpredictability of metabolism in vivo.

An exciting delivery system nanosuspensions, a sub-micro colloidal dispersion system developed by Müller et al. (1995a,b), can overcome the above limitations. In this system, pure drug particles are stabilized by small amount of surfactants and polymeric materials, and drugs existed in a nano-sized, pharmaceutically acceptable crystalline or amorphous state. A significant advantage of the nanosuspensions is that they can be given by various routes of administration, such as oral (Liversidge and Cundy, 1995), parenteral (Peters et al., 2000), ocular Rosario et al., 2002) and pulmonary pathways (Jacobs and Müller, 2002). In addition, a lot

* Corresponding author. Tel.: +86 24 23986321; fax: +86 24 23986321.
E-mail address: hezhonggui@gmail.com (Z. He).

0378-5173/$ – see front matter © 2009 Elsevier B.V. All rights reserved.
doi:10.1016/j.ijpharm.2009.05.062

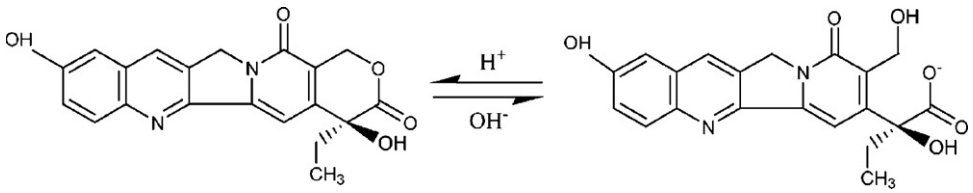

Fig. 1. The chemical structure of HCPT.

of studies demonstrated that nanosuspensions can enhance drug loading, dissolution rate and safety, and increase drug stability.

There are two general techniques for the production of drug nanosuspensions including 'bottom-up' and 'top-down' processes (Van Eerdenbrugh et al., 2007). In the bottom-up process nanoparticles grow up from the accumulation of drug molecules, which includes microprecipitation (Rogers et al., 2004; Matteucci et al., 2006, 2007), microemulsion (Trotta et al., 2001, 2003), and melt emulsification method (Kocbek et al., 2006). The top-down technologies employ the breaking down of large particles to form nanoparticles, which include high-pressure homogenization (Krause and Müller, 2001; Zhang et al., 2007c) and media milling method (Van Eerdenbrugh et al., 2007). In this study, we employed the combination of the above two techniques, microprecipitation and high-pressure homogenization method, to obtain small and uniform nanoparticles. For demonstrating that nanosuspensions can effectively protect 10-HCPT in its active form, the percentage of the lactone form in nanosuspensions versus that in the solution at different pH values was determined.

2. Materials and methods

2.1. Materials

10-HCPT (99% purity) was obtained from Huangshi Fy Pharmaceutical Co. Ltd. (China). Lutrol F 68 (poloxamer 188, a polyoxyethylene–polyoxyethylene tri-block copolymer) was kindly gifted by BASF (D-Ludwigshafen, Germany). Soybean phospholipid was purchased from BASF (D-Ludwigshafen, Germany). DMSO (Dimethyl sulfoxide) was supplied by Tianjin Concord Chemical Reagent Co. Ltd. (Tianjin, China). All other materials were purchased from Sigma (Hamburg, Germany).

2.2. Preparation of 10-HCPT nanosuspensions by microprecipitation–high-pressure homogenization method

10-HCPT nanosuspensions were prepared by the combination of microprecipitation and high-pressure homogenization method. Briefly, 20 mg F 68 was dissolved in 2 ml DMSO (the first solvent) by agitation and moderate heating, and then 20 mg 10-HCPT was added and stirred until dissolution followed by 15 min continuous agitation at 300 rpm at 70 °C. After the solution was cooled at room temperature, it was filtered through a 0.22 μm filter. Another solution was prepared by dispersing 20 mg soybean phospholipid in 100 ml water for injection (the second solvent) by high speed scatter homogenizer (Shanghai Specimen Model Factory, China). The first solution was then very quickly injected into the second one (the stabilizers solution) through a syringe with a 0.40 μm needle in an ice-water bathe at 3 °C. The second solution was stirred at 600, 1000, 4700 or 10,000 rpm respectively during the injection, and continuously stirred for 30 min after the injection was completed. Subsequently, the obtained pre-suspension was homogenized use an ATS AH110D homogenizer (ATS Engineer Inc. China). The homogenization process consists of two cycles at 200 bar and another two cycles at 500 bar as premilling, followed by several cycles at 600, 1000 or 1300 bar respectively to obtain the 10-HCPT nanosuspensions. 20 ml sample was collected for particle size analysis. The nanosuspensions were centrifuged at 16,000 × *g* for 15 min using a high speed centrifuge (TGL-16B, ShangHai Anting Scientific Instrument Factory, China). The volume of the supernatant was measured and replaced with fresh replacement solution including the same amount of soybean phospholipid and F 68. The sediment was redispersed using a high speed scatter homogenizer until no visible clumps were observed. The above replacement process was repeated for once more. A second homogenization was undertaken at the same pressure and cycles as the first homogenization to obtain the final nanosuspensions. This final nanosuspensions will be converted into the nanosuspension powders as the final product by lyophilization process (see Section 2.4).

2.3. Particle size analysis and zeta potential measurement

Particle size analysis of the nanosuspensions was performed by Laser diffraction (LD) using a Coulter LS 230 from Beckmann-Coulter Electronics (Krefeld, Germany). The nanosuspensions were diluted with water for injection to give an intensity of 300 Flux as recommended by the manufacturer. The zeta potential was measured using a Delsa 440SX Zeta Potential Analyzer (Beckmann-Coulter Electronics, Germany) with the nanosuspensions diluted in water for injection according to the manufacturer's manual.

2.4. Lyophilization

The 10-HCPT nanosuspensions were lyophilized using a Gamma 2-20 apparatus (Christ, Osterode A.H., Germany) for improving further the chemical and physical stability of the final product. The different amount of cryoprotectants (trehalose:mannitol, 1:1, w/w) were added into 2 ml of the nanosuspensions in 10 ml glass vials. The mixture was oscillated until the cryoprotectants were dissolved completely. The nanosuspensions were pre-frozen in the refrigerator (−25 °C and −75 °C) for 12 h and subsequently lyophilized at −25 °C for 24 h, followed by a secondary drying phase of 12 h at 20 °C.

2.5. Transmission electron microscopy (TEM)

The particle morphology and particle size of the 10-HCPT-nanosuspensions and 10-HCPT bulk drug were examined using TEM (H-600, Hitachi, Japan). The samples were stained with 2% (w/v) phosphotungstic acid for 30 s and placed on copper grids with films for viewing.

2.6. X-ray diffraction (XRD) measurements

Powder X-ray diffraction patterns were collected in transmission using an D/max 2400 X-ray diffractometer with a rotating anode (JEOL, Japan) with Cu Ka radiation (monochromator: graphite) generated at 200 mA and 40 kV. Powders of coarse 10-HCPT, mixture of soybean phospholipid, F 68, trehalose and mannitol (and "blank excipients"), lyophilized 10-HCPT-nanosuspensions, and physical mixture of soybean phospholipid, F 68 and 10-HCPT were respectively packed into the rotating sample holder between two films

(PETP). The obtained data were typically collected with a step width of 0.04° and a count time of 2 s.

2.7. Differential scanning calorimetry (DSC)

DSC analysis was performed using a TA-60 WS Thermal Analyzer (Shimadzu, Japan). For the DSC measurement, the same samples as XRD were weighed into an aluminum pan, which were then sealed with a pinhole-pierced cover. Heating curves were recorded at a scan rate of 10 °C/min from 30 to 300 °C.

2.8. Improvement of the stability of 10-HCPT lactone form

For studying the stability of 10-HCPT active lactone form in nanosuspensions in comparison to the 10-HCPT solution, the lactone form of 10-HCPT at different pH values was determined using HPLC. The determination method of the lactone form of 10-HCPT was developed by Liu et al. (2008). Briefly, 2.00 mg of 10-HCPT was dissolved in 100 ml of 0.1 mol/L NaOH, and 5 ml of the 10-HCPT solution was diluted to 25 ml with phosphate buffer saline (PBS) at different pH values (3.0, 5.0, 6.0, 7.0, 8.0) for the determination of the lactone form of the 10-HCPT solution. The contents of the lactone form at different pH were determined after the 24 h incubation at 4 °C. The content at pH 3.0 was defined as W_0, and the contents at other pH were defined as W_L. The percentage of the lactone form (E) was calculated from Eq. (1):

$$E(\%) = \frac{W_L}{W_0} \times 100 \quad (1)$$

For determination of the lactone form of 10-HCPT-nanosuspe nsions, the process was the same as the solution. The percentage of the lactone form (E) was also then calculated from Eq. (1).

2.9. In vitro dissolution test

Dissolution studies were carried out in a ZRS-8G drug dissolution apparatus (Tianjin University Radio Factory, Tianjin, China) by the paddle method of Chinese Pharmacopoeia 2005. The dissolution medium used was 600 ml of pH 7.4 phosphate buffer solution, which was incubated in a water bath at 37 °C. The rotation speed of the paddle was 75 rpm. A known amount of the aqueous suspension of drug nanoparticles or the reference coarse suspensions of 10-HCPT with F 68 and soybean phospholipid were added into the dissolution media. Approximately 2 ml samples were collected from the dissolution media at predetermined time points, filtered through a 0.1 μm syringe filter (Shanghai Huan'ao Trading Company, Shanghai, China). Then 50 μl phosphoric acid was added to 1 ml filtrate, then votexed for 2 min. The mixture was analyzed by the HPLC method. Sink conditions were maintained throughout the dissolution testing period. All dissolution experiments were performed in duplicates, and all sample analyses were carried out in triplicates.

2.10. HPLC analysis

HPLC analysis of 10-HCPT was performed on an Hitachi L-7200 series HPLC system (Hitachi, Japan) equipped with an autosampler system and a variable wavelength UV detector, with the detection wavelength set at 384 nm. Chromatographic separation was carried out with a Diamonsil C_{18} column (200 mm×4.6 mm, 5 μm; Dikma Technologies, China) eluted at a rate of 1.0 ml/min with mobile phase of methanol/PBS (pH 5.0) (3:2, v/v) at 35 °C. Standard solutions of 10-HCPT were prepared by diluting the appropriate volume of stock solution of 10-HCPT in methanol with methanol to give a final concentration of 0.1, 0.2, 0.5, 1, 2, 5 and 10 μg/ml. Then, 20 μL of the standard solutions was injected into the HPLC column. The peak area was obtained automatically by the Easy 3000 software (FULI Analytical Instrument Co., LTD. China). For HPLC analysis, the 10-HCPT nanosuspension samples could be obtained by dissolving the proper amount of nanosuspensions in 50 ml methanol.

Table 1
The several important parameters of the optimal process.

Items	Index
Agitation rate of stabilizer solution	1000 rpm
Temperature of stabilizer solution	<3 °C
Homogenization pressure	1000 bar
Homogenization cycle numbers	20 times

3. Results and discussion

3.1. Preparation of 10-HCPT nanosuspensions

In this study, we used a reproducible microprecipitation–high-pressure homogenization method to prepare 10-HCPT nanosuspensions, which minimized solvent residual due to replacement of the fresh stabilizer solution. During preparation, we have studied the effects of agitation rate, homogenization pressure and number of cycle on the particle size of the nanosuspensions. When the other process parameters were fixed, we changed the agitation rate for the stabilizer solution at 600, 1000, 4700 or 10,000 rpm and found the particle size has hardly changed when the agitation rate was over 1000 rpm (Fig. 2A) When homogenization pressure was changed in the range 600–1300 bar, the particle sizes of final nanosuspensions did not show obvious difference between 1000 and 1300 bar, but were larger at 600 bar (Fig. 2B). As the homogenization number of cycle is increased in the production process, the particle size firstly decreased and then increased slightly, with the smallest particle size observed after 20 homogenization cycles (Fig. 2C). As can be seen, the particle size of the final nanosuspensions was mainly affected by homogenization pressure and cycles. The role of agitation rate is relatively weak. Therefore, the optimal values of the agitation rate of stabilizer solution, homogenization pressure and number of cycle were selected as 1000 rpm, 1000 bar and 20 times, respectively (Table 1).

During the production process, microprecipitation was the first size-controlling step. It could change the crystal type and physical state of drug particles, and therefore decreased the energy required to produce the nanosuspensions and made homogenization process easier. The first homogenization process reduced drug particle size continuously, and it should help induce the absorption of surfactant onto drug particles, promoting an annealing effect which can increase stability of the nanosuspensions. In this study, aggregation was observed half hour after microprecipitation without homogenization; with homogenization, nanosuspensions could be stored for 6 months without any change (data not shown). Of course, this stability was also attributed to the reduced particle size by the homogenization.

3.2. Particle size, zeta potential and morphology

The mean particle sizes and zeta potentials of three batches 10-HCPT-nanosuspensions are presented in Table 2. The mean diameter of 10-HCPT-nanosuspensions was 131 nm. Zeta potential is essential to the storage stability of colloidal dispersion, and the mean zeta potential of the three batches 10-HCPT-nanosuspensions was −25.8 mV. The morphology of particle in nanosuspensions depended on the stabilizer used and drug concentration in the first solution, which had been already confirmed by other authors (Zhang et al., 2006b; Sinswat et al., 2007). In this study nanoparticles were claviform or columnar in shape, being similar to the

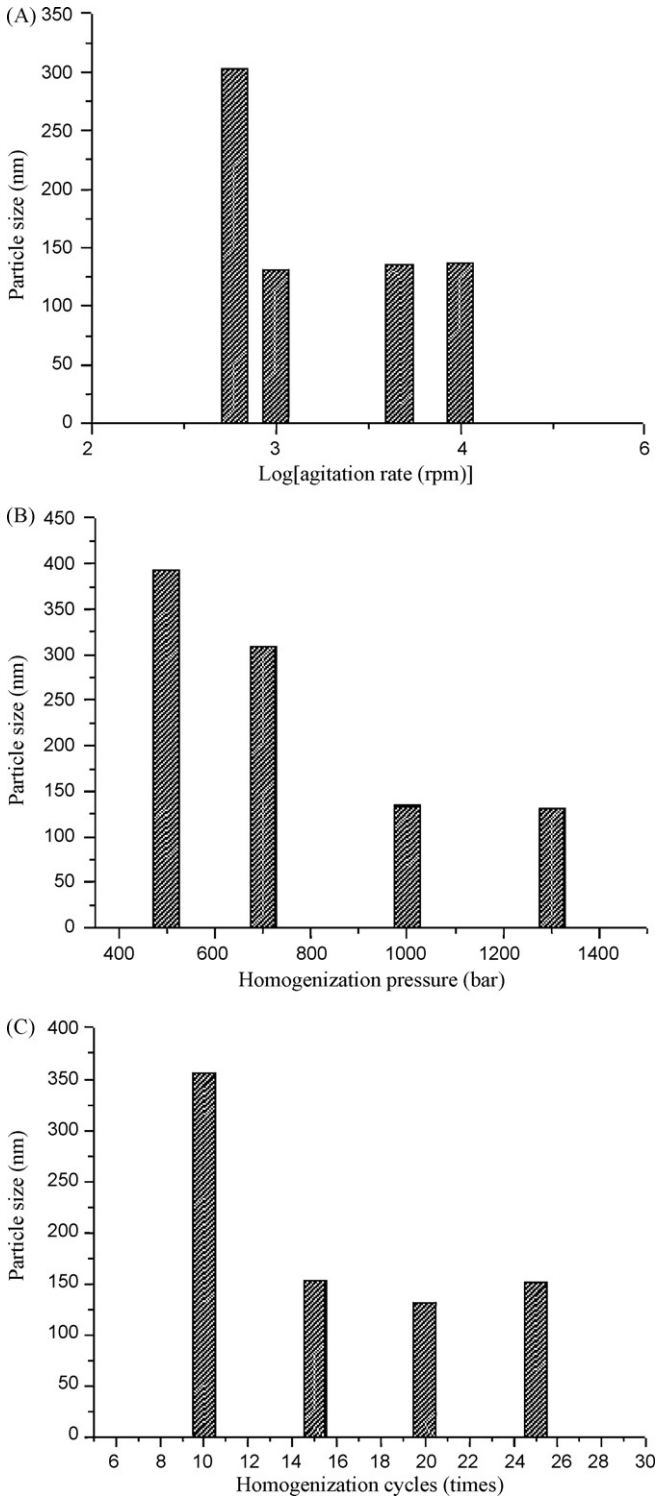

Fig. 2. Influence of the agitation rate of stabilizer solution (A), homogenization pressure (B) and homogenization cycles (C) on the particle size reduction of 10-HCPT nanosuspensions.

Table 2
The particle size and zeta potential of three batches nanosuspensions ($n = 3$).

Batch No.	Mean particle size (nm)	Size distribution (nm)			Zeta potential (mV)
		D_{10}	D_{50}	D_{90}	
20080915	131	108	130	156	−25.5
20080917	131	109	130	156	−25.3
20080920	129	107	128	153	−27.2

bulk drugs but the size was reduced by several times compared with bulk drugs (Fig. 3). The nanoparticle size observed by TEM was in good agreement with that by LD, which was almost below 200 nm. The microprecipitation–high-pressure homogenization method can achieve reproducible submicron-sized particles with a narrow distribution, and avoid or minimize the use of potentially toxic components.

3.3. X-ray diffraction (XRD) measurements

Fig. 4 showed the XRD patterns of 10-HCPT coarse powder, blank excipients, lyophilized nanosuspensions and physical mixture. The diffraction patterns of 10-HCPT coarse powders showed characteristic high-energy diffraction peaks at 2θ values between 6° and 30°, indicating the crystalline structure of 10-HCPT. In the physical mixture, the diffraction patterns of 10-HCPT was well consistent with that of the 10-HCPT coarse powders, indicating that 10-HCPT also existed in the crystalline form. In the lyophilized nanosuspensions, the sharp peaks of pure 10-HCPT were not observed, indicating the disappearance of crystalline structure in 10-HCPT nanosuspensions. This suggests that 10-HCPT may be present in an amorphous state in the lyophilized 10-HCPT nanosuspensions.

3.4. Differential scanning calorimetry (DSC)

The DSC study investigation (Fig. 5) gave similar results to the XRD study. The coarse drug powders exhibited a sharp melt process, with an onset temperature of 275.92 °C and a peak of 278.63 °C. In the physical mixture, the endothermic peak of 10-HCPT drifted 5.5 °C to the left, due to the mixing with soybean phospholipid and F 68. No melting process was observed for the lyophilized 10-HCPT nanosuspensions, indicating that there was no crystalline 10-HCPT in the lyophilized nanosuspensions and the transition of crystalline state to amorphous state may have taken place during the microprecipitation process. The formation of a high energy amorphous drug can increase C_{sat} compared to crystalline, coarse drug, so the faster dissolution profiles were expected.

3.5. Improvement of the stability of 10-HCPT lactone form

Here, the chemical stability of 10-HCPT referred to the reaction of lactone form of 10-HCPT transferring to the carboxylate form under illumination and at different pH values. As pH has been reported to be the most important factor to affecting the conformational conversion of 10-HCPT, the stability study of 10-HCPT lactone form was carried out at different pH values. The percentage of the active lactone form of 10-HCPT in solution and 10-HCPT nanosuspensions at different pH values is shown in Fig. 6. We found that with an increase in pH, the conversion of 10-HCPT was greatly increased in the solution as indicated by the lower percentage of 10-HCPT remained. At physiological pH values (pH 7.0–7.4), less than 30% of 10-HCPT was left after the 24 h incubation. However, nearly 90% of 10-HCPT in the nanosuspensions was preserved in the lactone form even at the least stable pH (8.0), clearly demonstrating the superiority of nanosuspensions to solution in terms of stability. This is higher than the 80% preservation rate in a lipid carrier reported by Liu et al. (2008), which suggested that the protective effect of nanosuspensions is better than that of nanostructured lipid carriers. Therefore it is clear that the nanosuspension delivery system could effectively protect the active lactone form and may consequently improve the activity and reduce the toxicity of 10-HCPT.

There were two reasons accounted for the improved chemical stability of 10-HCPT in the nanosuspensions: Firstly, 10-HCPT in the nanosuspensions was mostly in the solid core surrounded by surface-active agents, which was almost not affected by outside pH

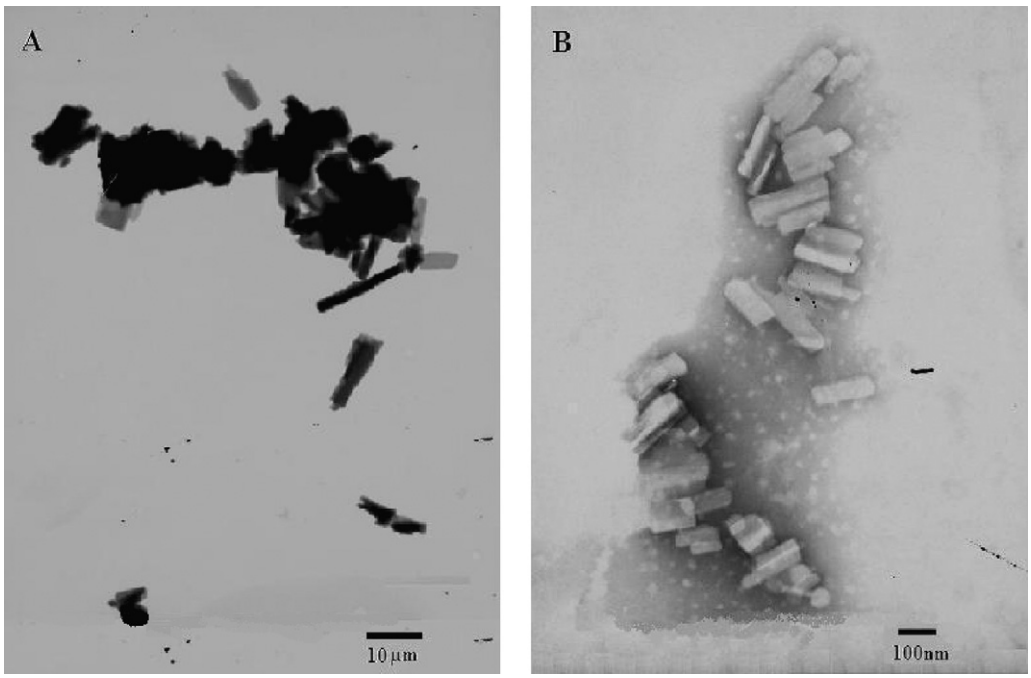

Fig. 3. The morphology of bulk 10-HCPT (A) and 10-HCPT nanosuspensions (B) observed using TEM.

values compared to the molecule form in solutions. Secondly, the rate of conversion from lactone form to the carboxylate form in solid state was very slow relative to that in solution, because of very low molecular mobility.

3.6. In vitro dissolution test

The micronization of poorly soluble drugs could increase the dissolution rate due to the increase in surface area but did not change the saturation solubility. When the particle size is reduced to the nanometer range, the solubility of drugs will increase significantly. The increase in solubility can be explained by the Ostwald–Freundlich equation:

$$\log\frac{C_s}{C_\infty} = \frac{2\nu\sigma}{2.303\,RT\rho r} \quad (2)$$

where C_s is the solubility, C_∞ is the solubility of the solid consisting of large particles, σ is the interfacial tension, ν is the molar volume of the particle material, R is the gas constant, T is absolute temperature, ρ is the density of the solid, and r is the radius of particles material (Müller and Peters, 1998).

According to Noyes–Whitney equation (see Eq. (3) below), the dissolution rate of a drug into an aqueous solution depends on the diffusion coefficient (D), the surface area (S), the equilibrium solubility of the drug (C_s), and the thickness of the diffuse layer (h):

$$\frac{dC}{dt} = \frac{DS}{h}(C_s - C) \quad (3)$$

where C is the concentration of the drug in bulk solution. So, an increase in C_s and surface area due to the reduction of particle size (large surface area, S) would result in an increased dissolution rate.

In this study, the dissolution rate of 10-HCPT nanosuspensions, in comparison with the 10-HCPT coarse suspensions, was investigated. Typical cumulative dissolution profiles were shown in

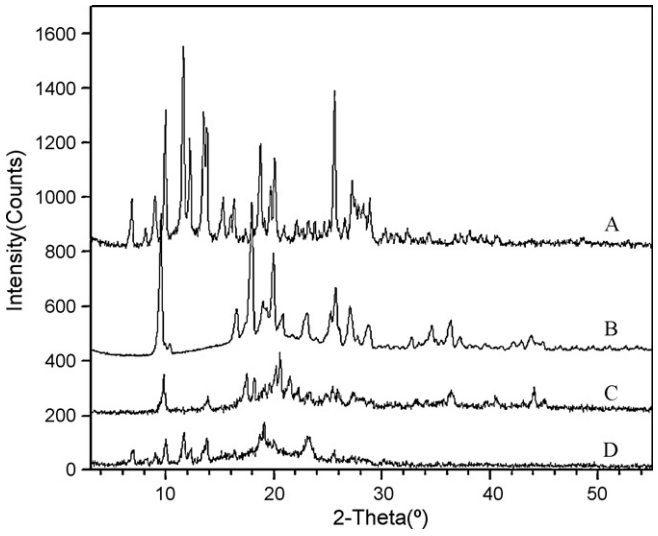

Fig. 4. The XRD patterns of bulk 10-HCPT (A), blank excipients (B), 10-HCPT nanosuspensions (C) and physical mixture (D).

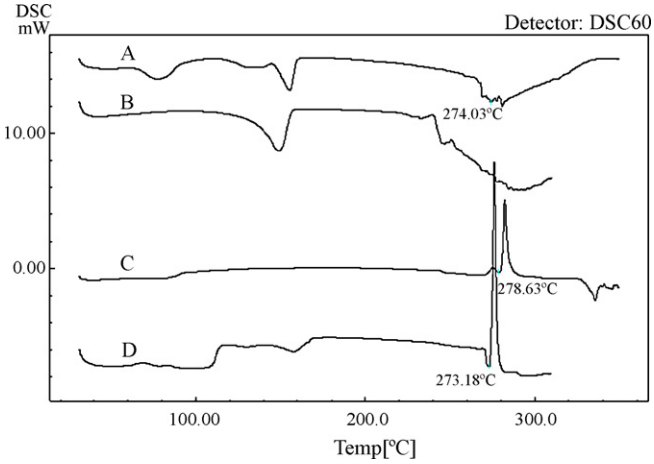

Fig. 5. Differential scanning calorimetry curves of blank excipients (A), lyophilized 10-HCPT nanosuspensions (B), bulk 10-HCPT crystalline powder (C) and physical mixture (D).

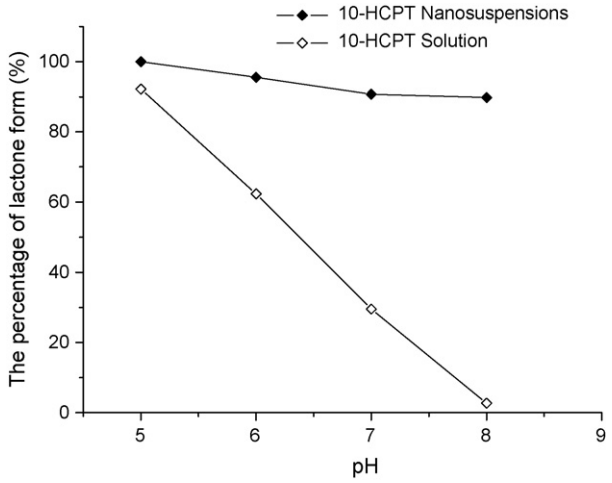

Fig. 6. The percentage of lactone form of 10-HCPT in the nanosuspensions (♦) and solution (◊) at different pH values after incubation at 4 °C for 24 h.

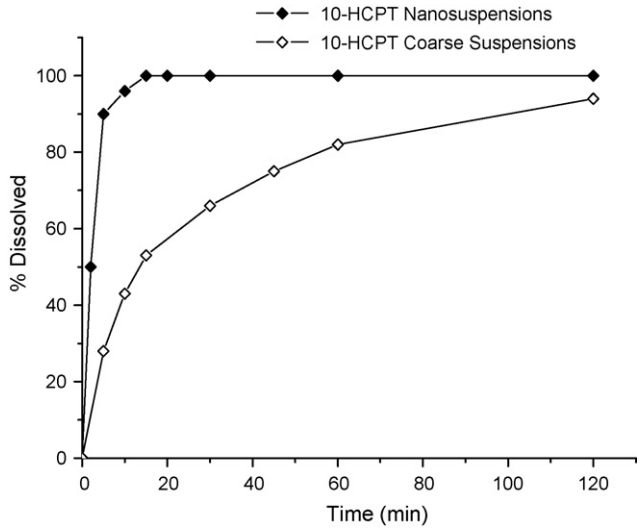

Fig. 7. Dissolution profiles of 10-HCPT nanosuspensions (♦) and 10-HCPT coarse suspensions (◊) in pH 7.4 phosphate buffer solution ($n = 3$).

Fig. 7. The dissolution rate was markedly enhanced in the nanosuspensions (131 nm), and nearly 100% of the drug dissolved within 15 min, as opposed to only 53% for the coarse 10-HCPT suspensions (7.369 μm). This could be attributed to the increased surface area and enhanced saturation solubility of 10-HCPT in the nanosuspensions. Therefore, formulating the poorly water-soluble 10-HCPT as nanometer-size nanosuspensions had a dramatic effect on the drug solubility, dissolution rate.

4. Conclusions

The microprecipitation–high-pressure homogenization technique was employed successfully to fabricate the 10-HCPT nanosuspensions. The particle size of nanoparticles is highly dependent on homogenization parameters. By employing optimized homogenization pressure and number of cycles, nanosuspensions with mean diameters below 200 nm and with very low polydispersity could be prepared.

There was a remarkable improvement of stability of 10-HCPT active form in nanosuspensions compared to the 10-HCPT solution at pH 7.0–8.0. The increased chemical stability could help to improve the activity and reduce the toxicity of 10-HCPT. This novel delivery system has a promising potential as an alternative parenteral formulation for 10-HCPT.

Acknowledgements

We are grateful for financial support from the National Basic Research Program of China (973 Program), No. 2009CB930300.

References

Guo, R., Zhang, L.Y., Jiang, Zh.P., Cao, Y., Ding, Y., Jiang, X.Q., 2007. Synthesis of alginic acid-poly[2-(diethylamino)ethyl methacrylate] monodispersed nanoparticles by a polymer–monomer pair reaction system. Biomacromolecules 8, 843–850.
Han, R., 1994. Highlight on the studies of anticancer drugs derived from plants in China. Stem Cells 12, 53–63.
He, X.G., Lu, W., Jiang, X.Q., Zhang, X.W., Ding, J., 2004. Synthesis and biological evaluation of bis and monocarbonate prodrugs of 10-hydroxycamptothecins. Bioorg. Med. Chem. 12, 4003–4008.
Hong, M.H., Zhu, S.J., Jiang, Y.Y., Tang, G.T., Pei, Y.Y., 2009. Efficient tumor targeting of hydroxycamptothecin loaded PEGylated niosomes modified with transferrin. J. Control. Release 133, 96–102.
Jacobs, C., Müller, R.H., 2002. Production and characterization of a budesonide nanosuspension for pulmonary administration. Pharm. Res. 19, 189–194.
Kocbek, P., Baumgartner, S., Kristl, J., 2006. Preparation and evaluation of nanosuspensions for enhancing the dissolution of poorly soluble drugs. Int. J. Pharm. 312, 179–186.
Krause, K., Müller, R.H., 2001. Production and characterization of highly concentrated nanosuspensions by high pressure homogenization. Int. J. Pharm. 214, 21–24.
Liu, K., Sun, J., Wang, Y.J., He, Y., Gao, K., He, Z.H., 2008. Preparation and characterization of 10-hydroxycamptothecin loaded nanostructured lipid carriers. Drug Dev. Ind. Pharm. 34, 465–471.
Liversidge, G.C., Cundy, K.C., 1995. Particle size reduction for improvement of oral bioavailability of hydrophobic drugs. I. Absolute oral bioavailability of nanocrystalline danazole in beagle dogs. Int. J. Pharm. 127, 91–97.
Lu, B., Zhang, Z.Q., 2006. Novel colon-specific microspheres with highly dispersed hydroxycamptothecin cores: their preparation, release behavior, and therapeutic efficiency against colonic cancer. J. Pharm. Sci. 95 (12), 2619–2630.
Matteucci, M.E., Brettmann, B.K., Rogers, T.L., Elder, E.J., Williams III, R.O., Johnston, K.P., 2007. Design of potent amorphous drug nanoparticles for rapid generation of highly supersaturated media. Mol. Pharm. 4 (5), 782–793.
Matteucci, M.E., Hotze, M.A., Johnston, K.P., Williams III, R.O., 2006. Drug nanoparticles by antisolvent precipitation: mixing energy versus surfactant stabilization. Langmuir 22 (21), 8951–8959.
Müller, R.H., Peters, K., 1998. Nanosuspensions for the formulation of poorly soluble drugs: preparation by a size reduced technique. Int. J. Pharm. 160, 229–237.
Müller, R.H., Peters, K., Becker, R., Kruss, B., 1995a. Nanosuspensions—a novel formulation for the i.v. administration of poorly soluble drugs. In: 7th Int. Conf. on Pharm. Technol. (APV:APGI), Budapest, pp. 491–492.
Müller, R.H., Peters, K., Becker, R., Kruss, B., 1995b. Nanosuspensions for the i.v. administration of poorly soluble drugs—stability during sterilization and long-term storage. In: 22nd Int. Symp. Control. Release Bioact. Mater, Seattle, pp. 574–575.
Peters, K., Leitzke, S., Diederichs, J.E., Borner, K., Hahn, H., Müller, R.H., Ehlers, S., 2000. Preparation of clofazamine nanosuspension for intravenous use and evaluation of its therapeutic efficacy in *Mycobacterium avium* infection. J. Antimicrob. Chem. 45, 77–83.
Rogers, T.L., Nelsen, A.C., Brown, J.N., Fransen, K.L., Crowl, C.A., Tucker, C.J., Kupperblatt, G.B., Becker, J.N., Wilson, D.L., Todd, C., Broomall, C.F., Evans, J.C., Elder, E.J., 2004. Development and characterization of a scalable controlled precipitation process to enhance the dissolution of poorly water-soluble drugs. Pharm. Res. 21 (11), 2048–2057.
Rosario, P., Claudio, B., Piera, F., Adriana, M., Antonina, P., Giovanni, P., 2002. Eudragit RS100 nanosuspensions for the ophthalmic controlled delivery of ibuprofen. Eur. J. Pharm. Sci. 16, 53–61.
Shenderova, A., Burke, T.G., Sehwendeman, S.P., 1997. Stabilization of 10-hydroxycamptothecin in poly(lactide-co-glycolide) microsphere delivery vehicles. Pharm. Res. 14 (10), 1406–1414.
Shenderova, A., Burke, T.G., Sehwendeman, S.P., 1999. The acidic microelimate in poly(lactide-co-glycolide) microspheres stabilizes camptothecins. Pharm. Res. 16 (2), 241–248.
Shi, B., Fang, C., Pei, Y.Y., 2006. Stealth PEG-PHDCA niosomes: effects of chain length of peg and particle size on niosomes surface properties, in vitro drug release, phagocytic uptake, in vivo pharmacokinetics and antitumor activity. J. Pharm. Sci. 95 (9), 1873–1887.
Sinswat, P., Matteucci, M.E., Johnston, K.P., Williams III, R.O., 2007. Dissolution rates and supersaturation behavior of amorphous repaglinide particles produced by controlled precipitation. J. Biomed. Nanotechnol. 3, 18–27.
Slichemeyer, W.J., Rowinsky, E.K., Donehower, R.C., Kaufmann, S.H., 1993. The current status of camptothecin analogues as antitumor agents. J. Natl. Cancer. Inst. 85, 271–291.
Sun, X., Wu, F., Lu, W., Zhang, Zh.R., 2004. Sustained-release hydroxycamptothecin polybutylcyanoacrylate nanoparticles as a liver targeting drug delivery system. Pharmazie 59 (10), 791–794.

Trotta, M., Gallarat S e.M., Carlotti, M.E., Morel, S., 2003. Preparation of griseofulvin nanoparticles from water-dilutable microemulsions. Int. J. Pharm. 254, 235–242.
Trotta, M., Gallarate, M., Pattarino, F., Morel, S., 2001. Emulsions containing partially water miscible solvents for the preparation of drug nanosuspensions. J. Control. Release 76, 119–128.
Van Eerdenbrugh, B., Froyen, L., Martens, J.A., Blaton, N., Augustijns, P., Brewster, M., Van den Mooter, G., 2007. Characterization of physico-chemical properties and pharmaceutical performance of sucrose co-freeze-dried solid nanoparticulate powders of the anti-HIV agent loviride prepared by media milling. Int. J. Pharm. 338, 198–206.
Wall, M.E., Wani, M.C., Cook, C.E., Palmer, K.H., McPhail, A.T., Sim, G.A., 1966. Plnat antitumor agent. 1. The isolation and structure of camptothecin, a novel alkaloidal leukemia and tumor inhibitor from camptotheca acumianta. J. Am. Chem. Soc. 88 (16), 3888–3890.
Wang, Y.Q., Li, L.F., Jiang, W., Larrick, J.W., 2005. Synthesis and evaluation of a DHA and 10-hydroxycamptothecin conjugate. Bioorg. Med. Chem. 13, 5592–5599.
Hsiang, Y.H., Hertzberg, R., Hecht, S., Liu, L., 1985. Camptothecin induces protein-linked DNA breaks via mammalian DNA topoisomerase I. J. Biol. Chem. 260 (27), 14873–14878.
Yang, L., Cui, F.D., Cun, D.M., Tao, A.J., Shi, K., Lin, W.H., 2007. Preparation, characterization and biodistribution of the lactone form of 10-hydroxycamptothecin (HCPT)-loaded bovine serum albumin (BSA) nanoparticles. Int. J. Pharm. 340, 163–172.
Zhang, L.Y., Yang, M., Wang, Q., Li, Y., Guo, R., Jiang, X.Q., Yang, Ch.Zh., Liu, B.R., 2007a. 10-Hydroxycamptothecin loaded nanoparticles: preparation and antitumor activity in mice. J. Control. Release 119, 153–162.
Zhang, C., Ding, Y., Yu, L.L., Ping, Q.N., 2007b. Polymeric micelle systems of hydroxycamptothecin based on amphiphilic *N*-alkyl-*N*-trimethyl chitosan derivatives. Colloid Surf. B 55, 192–199.
Zhang, D.R., Tan, T.W., Gao, L., Zhao, W.F., Wang, P., 2007c. Preparation of Azithromycin nanosuspensions by high pressure homogenization and its physicochemical characteristics studies. Drug Dev. Ind. Pharm. 33, 569–575.
Zhang, L.Y., Sun, M.J., Guo, R., Jiang, Zh.P., Liu, Y., Jiang, X.Q., Yang, Ch.Zh., 2006a. Chitosan surface-modified hydroxycamptothecin loaded nanoparticles with enhanced transport across caco-2 cell monolayer. J. Nanosci. Nanotechnol. 6, 2912–2920.
Zhang, X., Xia, Q., Gu, N., 2006b. Preparation of all-trans retinoic acid nanosuspensions using a modified precipitation method. Drug Dev. Ind. Pharm. 32, 857–863.
Zhao, Y.X., Gao, J.Q., Sun, X.Y., Chen, H.L., Wu, L.M., Liang, W.Q., 2007. Enhanced nuclear delivery and cytotoxic activity of hydroxycamptothecin using o/w emulsions. J. Pharm. Pharmaceut. Sci. 10 (1), 61–70.